Field Measurement and End Shim Control of the HIMAC Quadrupole Magnet

Akifumi ITANO, Masayuki KUMADA, Kenji SATO, Kouji NODA,
Eiichi TAKADA, Mitsutaka KANAZAWA and Michio SUDOU
NIRS, National Institute of Radiological Sciences
9-1, Anagawa, 4-Chome, Inage-ku, Chiba-shi, Chiba-ken 263, JAPAN

Kuninori ENDO
KEK, National Laboratory for High Energy Physics
Oho 1-1, Tsukuba-shi, Ibaraki-ken 305, JAPAN

Hiroaki SAKURABATA and Tsuneyuki TONOOKA
Hitachi Works, Hitachi, Ltd.
1-1, Saiwai-cho 3-chome, Hitachi-shi, Ibaraki-ken 317, JAPAN

Abstract

The main quadrupole magnets of the HIMAC synchrotron ring have demountable pole end pieces made of glued stack of lamination silicon steel. Step-wise end cut was applied to the pole end pieces.

We measured the integrated field gradient distribution dBly(x)/dx by long twin search coil system. We analyzed how the output voltage from the twin coil changed with an addition or an omission of lamination sheets at different step positions. We could finally adjust the integrated field gradient distribution dBly(x)/dx to have a wide horizontal aperture x= ±122 mm.

I. INTRODUCTION

The HIMAC is a Heavy Ion Medical Accelerator for cancer therapy in Chiba at NIRS. The HIMAC synchrotron accelerates ion beams from He to Si(Ar) with charge to mass ratio q/A=0.5 up to 800 MeV/u corresponding to a magnetic rigidity Bρ= 9.75 T·m. The synchrotron ring is a separated function type with a strong FODO focusing structure and with a six-fold symmetry. Further details of the HIMAC synchrotron are described elsewhere [1], [2].

In the present paper, the main quadrupole magnets of HIMAC synchrotron and their field measurement are described. The method and results of the shim control of the integrated gradient field distribution are presented.

II. QUADRUPOLE MAGNET

The main quadrupole magnet system of the synchrotron ring is composed of 12 focusing magnets and 12 defocusing magnets.

The maximum integrated field gradient dBly/dx is 3 T. As the ring is designed to accelerate ion beams at a rate of dB/dt= 2 T/sec for the main dipole magnets [3], the magnet yokes are fabricated from stamped silicon steel lamination sheets of 0.5 mm thickness to reduce eddy current effects. The steel used is 50A600 of Nippon steel corporation. Coercitivity Hc is 65.30 ± 2.28 A/m. Magnetic induction field B_{50} at 5000A/m of magnetic field strength is 1.680 ± 0.003 T.

The pole shape was determined by a computer code TRIM. It is of hyperbolic shape with a tangential extension at both sides to have a wide flat region of field gradient distribution. Width of the yoke is set to be less than the height to make a space for a beam extraction line. Table 1 summarizes the specifications of the quadrupole magnet.

The magnets have demountable pole end pieces made of glued stack of lamination silicon steel that are fixed to the magnet yoke by screw bolts. This enabled an experimental determination of the end shim to control the integrated field gradient distribution. Step-wise end cut is applied to the pole end pieces. Outer parts of 30 mm length at both ends of the magnet yoke are also glued to have a solid plane to attach the pole end pieces.

III. FIELD MEASUREMENT AND END SHIM CONTROL

We measured the integrated field gradient distribution dBly(x)/dx by long twin search coil system. Turn number of each coil is 1152. Each coil of the twin search coil system was calibrated in a uniform region of the HIMAC dipole magnet that was calibrated by NMR system. The effective area of the coils was thus obtained. The length of each coil was 1002.5 mm. Widths of left and right coils of the twin coil were then deduced to be 7.04 mm and 7.09 mm, respectively. Distance between two coils was obtained by a field measurement in the quadrupole magnet. Absolute field distribution Bly(x) in quadrupole magnet was measured using one coil of the twin coil. The result was compared with a field gradient output of the twin coil. The distance was 11.38 mm.

Output signal from the twin coil was integrated by a temperature controlled integrator with a time constant RC= 0.33 sec. Integrator outputs and magnet currents were measured before and after magnet excitation. Initialization of the hysteresis loop of the magnet was performed before measurement.

We fabricated pole end pieces whose end cut steps approximated a line with tangent 1.4 with respect to the beam axis[4]. Table II gives width W and height H of each step of the initial end shim. Step #a indicates a side that is attached to the magnet yoke. Width of each step is 4 mm. Fig. 2 shows the integrated field gradient distribution for the initial end shim at excitation currents 400A and 1350A. These currents correspond to the acceleration energy range 100 - 800 MeV/u where beams are extracted. The results show that the distribution has a deviation larger than $1x10^{-2}$. This gives a large octupole component in the magnetic field. The result is that an outgoing trajectory of the phase space separatrix in slow extraction process is distorted and that a beam will not be extracted.

As measurements with different tangent values did not give a required aperture, we measured systematically how the output voltage distribution from the twin coil changed when we added or omitted lamination sheets at different steps of the end shim. The output voltage change had different x-distribution with different step position of the added or omitted lamination sheet. It seems that hyperbolic magnetic flux lines passing around the cross point between an end cut line and a hyperbolic pole face are affected most when we changed its step width. Back-side steps (side #a) give a larger change at central part of the distribution. Front-side steps (side #f) give a larger change at outer part of the distribution. As examples, Fig. 2 - 3 shows the changes of output voltage distribution when we changed the widths of step #c and #f by -1 mm and

TABLE I
Specifications of the HIMAC Quadrupole Magnet

Number / ring	12 Focusing
	12 Defocusing
Maximum field gradient	7 T / m
Maximum integrated gradient	3 T
Aperture diameter	192 mm
Magnet length	400 mm
Good field region Hor / Ver	244 mm / 56 mm
Magnet yoke size	900^{w} x 980^{h} x400^{l} mm
Number of coil turns / pole	18
Maximum current	1360 A
Coil resistance	9.7 mΩ
Coil inductance	9.2 mH
Magnet weight	3.2 ton
Cooling water flow	18 l / min.
Magnet yoke material	laminated silicon steel
	Nippon steel corporation
	50A600
Lamination thickness	0.5 mm

TABLE II
Width and Height of each step of the end pole piece in mm.

Step No.	#a	#b	#c	#d	#e	#f
Initial W	4	4	4	4	4	
H	0	7	12.5	18	23.5	
Final W	4	4	1	3	5	4
H	0	7	12.5	18	23.5	30

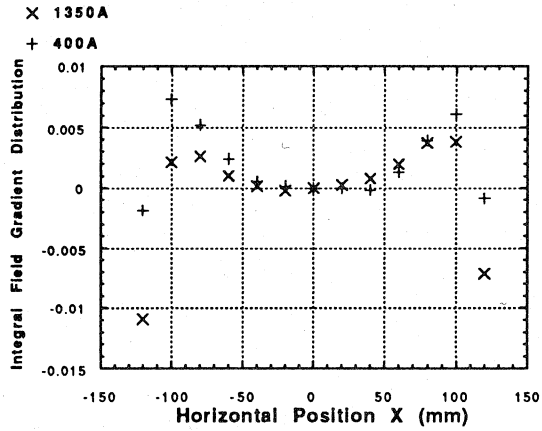

Fig. 1. Normalized integrated field gradient distribution for initial end shim at excitation current 1350A and 400A. The distribution is not satisfactory.

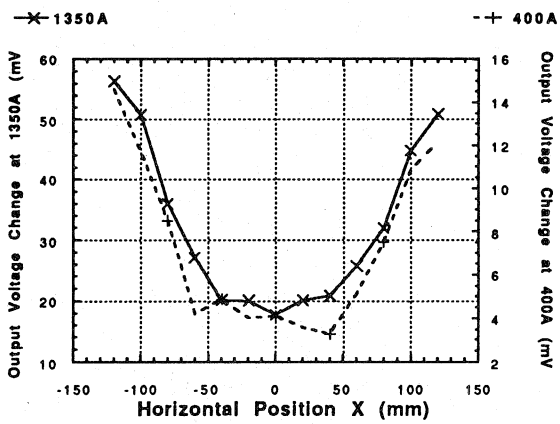

Fig. 2. Change of output voltage for 1 mm width change of step #c.

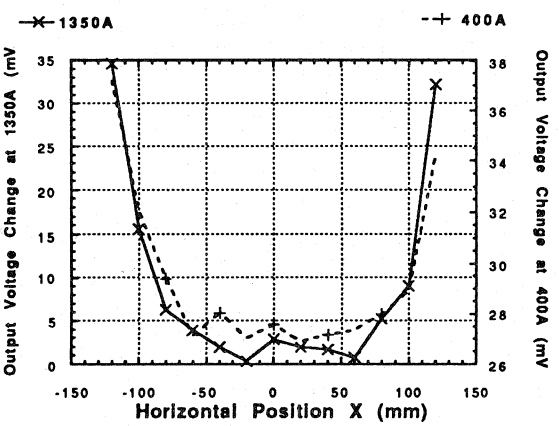

Fig. 3. Change of output voltage for 1 mm width change of step #f.

+1 mm respectively at excitation current 400A and 1350A. Having known the voltage changes for unit change of width for each step, we could calculate a voltage distribution for a new pattern of end shim. So we could determine a new form of the end cut for a desired gradient distribution. However, as the end pieces have a saturation at edge and the field has a component perpendicular to the lamination sheet, the procedure was not so straight forward when we changed widths of several steps at a same time. We needed some iterations to obtain the result. Fig. 4 compares observed output voltage distributions (in mV) for initial end shim, one of intermediate end shims and final end shim at 1350 A. Fig. 4 also shows a prediction for final end shim. Although there was a slight discrepancy between prediction and observation, we could finally adjust the integrated field gradient distribution dBly(x)/dx to have a required horizontal aperture x= ±122 mm.

Fig. 5 shows a pattern of the final end shim. Table II summarizes width and height of each step. Fig. 6 shows the resultant integrated field gradient distribution. Deviations are less than 8×10^{-3} and 3×10^{-3} at 400A and 1350A, respectively.

Fig. 7 shows an excitation of the integrated field gradient Glo = dBly(x=0)/dx in Tesla. The relative deviation of the magnet strength among the whole magnets at full excitation current 1350A is ±0.3 %.

IV. References

[1] Y.Hirao et al., "Heavy Ion Medical Accelerator in Chiba - A Design Summary and Update - ", NIRS-M-89 and HIMAC-001, December 1992 and references therein.

[2] K.Sato et al., "Present status of NIRS medical accelerator - HIMAC." in these proceedings.

[3] A.Itano et al., Proc. 8th Sym. Accel. Sci. Tech., RIKEN, Saitama, Japan (1991) 202.

[4] M.Kumada et al., Nucl. Instr. and Methods, 211(1983)283.

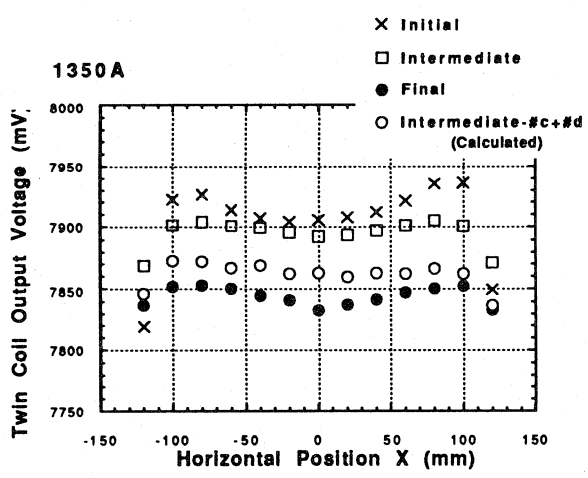

Fig. 4. Twin coil output voltages for different end shims. Calculated distribution is a prediction for the final end shim and is compared with observed final distribution.

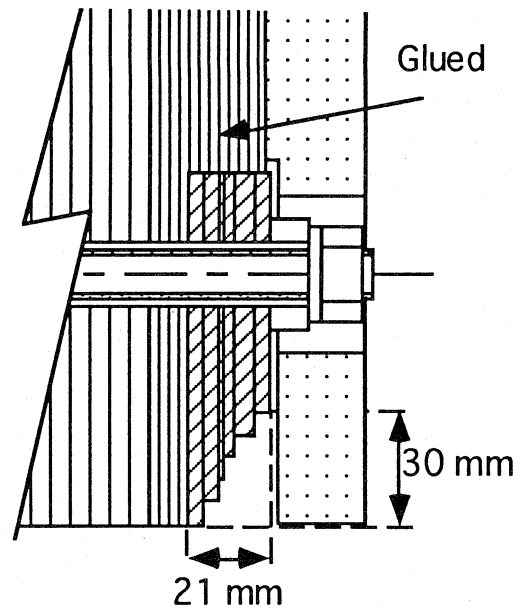

Fig. 5. Final end shim.
This end shim gave a satisfactory result.

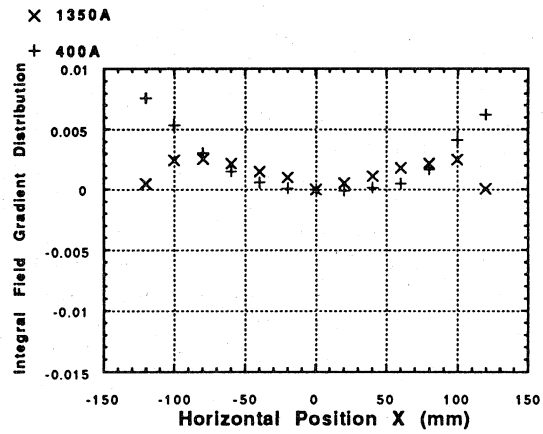

Fig. 6. Normalized integrated field gradient distribution for a final end shim at excitation current 1350A and 400A.

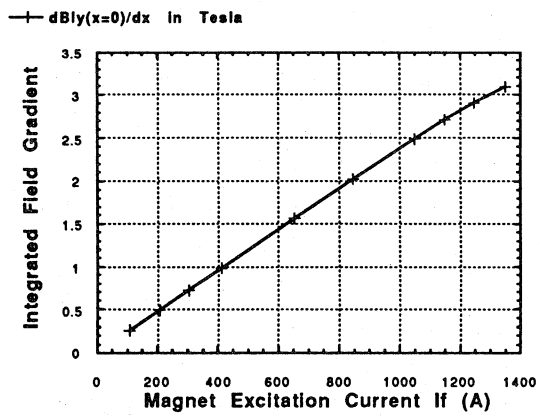

Fig. 7. Excitation of the integrated field gradient in Tesla.